

Reduction of gap and adherens junction proteins and intercalated disc structural remodeling in the hearts of mice submitted to severe cecal ligation and puncture sepsis*

Mara Rúbia N. Celes, MSc; Diego Torres-Dueñas, MD, PhD; José C. Alves-Filho, MSc; Djane B. Duarte, MSc; Fernando Q. Cunha, PhD; Marcos A. Rossi, MD, PhD

Objective: The present study describes intercalated disc remodeling under both protein expression and structural features in experimental severe sepsis induced by cecal ligation and puncture in mice.

Design: Controlled animal study.

Setting: University research laboratory.

Subjects: Male C57BL/6 mice.

Interventions: Mice were submitted to moderate and severe septic injury by cecal ligation and puncture.

Measurement and Main Results: Severe septic injury was accompanied by a large number of bacteria in the peritoneal cavity and blood, high levels of tumor necrosis factor- α , and monocyte inflammatory protein-1 α in the septic focus and serum, marked hypotension, and a high mortality rate. Western blot analysis and immunofluorescence showed a marked decrease of key gap and adherens junction proteins (connexin43 and N-cadherin, respectively) in mice submitted to severe septic injury. These changes may result in the

loss of intercalated disc structural integrity, characterized in the electron microscopic study by partial separation or dehiscence of gap junctions and adherens junctions.

Conclusions: Our data provide important insight regarding the alterations in intercalated disc components resulting from severe septic injury. The intercalated disc remodeling under both protein expression and structural features in experimental severe sepsis induced by cecal ligation and puncture may be partly responsible for myocardial depression in sepsis/septic shock. Although further electrophysiological studies in animals and humans are needed to determine the effect of these alterations on myocardial conduction velocity, the abnormal variables may emerge as therapeutic targets, and their modulation might provide beneficial effects on future cardiovascular outcomes and mortality in sepsis. (Crit Care Med 2007; 35:2176–2185)

KEY WORDS: sepsis; myocardial depression; adherens junction; cell adhesion; intercalated disc

The intercalated disc maintains the structural integrity of the heart by the end-to-end connection of myocytes. The myocardial contractile function depends on intercalated discs for mechanical and electrical/chemical coupling of cardiomy-

ocytes. The intercalated disc contains various junctional complexes: adherens junctions, desmosomes, and gap junctions (1, 2). Adherens junctions, consisting of cadherins, link the intercalated disc to the actin cytoskeleton, and desmosomes, mainly composed of desmoplakin, attach to the intermediate filaments. Both associate with catenin complex proteins to regulate the cell-to-cell adhesion and the structure of the junctions at the intercalated disc, enabling the transmission of the contractile force across the plasma membrane. Gap junctions, consisting of connexons composed of six connexin proteins extending across cell membranes, provide intercellular communication between neighboring cardiomyocytes via electrical stimulus and ion transfer.

It is known that disruption of intercalated disc constituent proteins give rise to cardiomyopathy and other fatal defects (3). For example, induced deletion of the N-cadherin gene in the heart of mice leads to loss of intercalated disc struc-

tures, resulting in abnormal cardiac morphology and function (4). Remodeling of gap-junction organization and reduction of the levels of the predominant connexin of the heart ventricle, connexin43, has been shown to result in slow conduction velocity, spontaneous ventricular arrhythmia, and sudden cardiac death (5–8). In Naxos disease, an arrhythmogenic right ventricular cardiomyopathy due to deletion of plakoglobin, a remodeling of gap junctions has been shown, probably due to abnormal linkage between desmosomes and adherens junctions and the cytoskeleton (9).

Cardiac dysfunction due to impaired myocardial contractility has been recognized as an important factor contributing to high mortality in septic patients (10). Recent study from our laboratory gives support to the opinion that myocardial structural change, classifiable as inflammatory cardiomyopathy, could be responsible for sepsis-induced myocardial dysfunction (11). The present study describes intercalated disc remodeling under both

*See also p. 2231.

From the Departments of Pathology (MRNC, MAR) and Pharmacology (JCAF, DBD, FQC), Faculty of Medicine of Ribeirão Preto, University of São Paulo, Ribeirão Preto, São Paulo, Brazil; and the Department of Pharmacology, Faculty of Medicine, Autonomous University of Bucaramanga, Bucaramanga, Colombia (DTD).

The authors have not disclosed any potential conflicts of interest.

Supported, in part, by grants 04/01777-0 and 04/14578-5 from the Fundação de Amparo à Pesquisa do Estado de São Paulo, Brazil, and the Conselho Nacional de Desenvolvimento Científico e Tecnológico, Brazil.

For information regarding this article, E-mail: marossi@fmrp.usp.br

Copyright © 2007 by the Society of Critical Care Medicine and Lippincott Williams & Wilkins

DOI: 10.1097/01.CCM.0000281454.97901.01

protein expression and structural features in experimental severe sepsis induced by cecal ligation and puncture (CLP) in mice. These findings make plausible the hypothesis that alterations in cell communication and mechanical coupling between neighboring cardiomyocytes could contribute to myocardial depression in sepsis.

MATERIALS AND METHODS

Animals. Male C57BL/6 mice (average weight, 22 g) were acclimated to the laboratory environment for 24–48 hrs before experimentation and received H₂O and food *ad libitum*. The mice were maintained at 22 ± 2°C on a 24-hr day/night cycle, with 12 hrs of light and 12 hrs of darkness. The animal experiments performed in the present study were conducted according to the guidelines of the Animal Care Committee of the Faculty of Medicine of Ribeirão Preto, and the experimental protocols were approved by the Committee.

Sepsis Model. Sepsis was induced through CLP. Briefly, mice were anesthetized with 250 mg/kg tribromoethanol intraperitoneally. A 1-cm midline incision was made, and the cecum was exposed and ligated with 5-0 silk below the ileocecal junction without causing bowel obstruction. A single puncture was made through the cecum using a 30-gauge or an 18-gauge needle to induce moderate septic injury (MSI) and severe septic injury (SSI), respectively. The cecum was then replaced in its original position and the abdomen sutured. Each animal received a subcutaneous injection of 1 mL of 0.9% NaCl solution (37°C) and maintained under the conditions stated above.

Number of Bacteria in the Peritoneal Cavity and Blood. Six hours after surgery, the mice were killed. For bacterial count in the peritoneal cavity, the abdominal skin was thoroughly disinfected, and 2 mL of sterile phosphate-buffered saline was injected into and 1 mL aspirated out of the peritoneal cavity. Aliquots of serial log dilutions of the peritoneal aspirate were plated on Mueller-Hinton agar dishes (Difco Laboratories, Detroit, MI) and incubated at 37°C for 24 hrs. Colony-forming units (CFU) were then counted and expressed as the log of CFU per peritoneal cavity. For bacteremia, blood was collected under sterile conditions and 10 µL collected and plated on Mueller-Hinton agar dishes (Difco). CFU were counted 24 hrs after incubation at 37°C and the results expressed as the log of CFU per milliliter of blood.

Measurement of Carotid Blood Pressure. Carotid artery blood pressure was obtained in anesthetized animals (250 mg/kg tribromoethanol intraperitoneally) 6, 12, and 24 hrs after surgery. A catheter was positioned in the right carotid artery and exteriorized in the neck. When hemodynamics became stable, mean carotid pressure was recorded by connecting the catheter to the pressure transducer (Powerlab, AD Instruments, Castle Hill,

Australia). Mean carotid pressure of anesthetized animals, simulating the time 0 of the experiment immediately before surgery, was also measured.

Cytokine and Chemokine Measurements. Six hours after CLP, the concentrations of tumor necrosis factor-α (TNFα) and monocyte inflammatory protein-1α (MIP-1α) in the peritoneal exudate and serum were determined by using a double-ligand enzyme-linked immunosorbent assay. The results were expressed as picograms of TNFα or MIP-1α per milliliter of supernatant or serum. Recombinant murine TNFα and MIP-1α standard curves were used to calculate the cytokine concentrations.

Western Blot. To determine the amounts of connexin43 and N-cadherin in septic hearts, homogenates of left and right ventricles were analyzed by immunoblotting 24 hrs after surgery. Freshly excised hearts were washed in cold phosphate-buffered saline, and the left and right ventricles were isolated and homogenized in extraction buffer and protease inhibitor cocktail (Sigma-Aldrich, St. Louis, MO). Total heart protein (40 µg protein/well) was resolved on 7% or 12% sodium dodecyl sulfate-polyacrylamide gel electrophoresis and transferred to nitrocellulose membrane (Hybond-ECL, Amersham Pharmacia Biotech, Amersham, UK). The membranes were blocked with 5% skimmed milk/Tris-buffered saline with 0.1% Tween 20 for 24 hrs and incubated overnight at 4°C with the primary antibodies (goat polyclonal anti-N-cadherin, 1:500; mouse monoclonal anti-connexin43, 1:500; Santa Cruz Biotechnology, Santa Cruz, CA). The blots were washed and incubated with horseradish peroxidase-conjugated secondary antibodies (rabbit anti-goat immunoglobulin G, 1:20,000; and horse anti-mouse immunoglobulin G, 1:7,000; Vector Laboratories, Burlingame, CA) for 1 hr at room temperature. The same antibodies were used for Western blot and immunofluorescence. The anti-connexin43 antibody recognizes both phosphorylated and nonphosphorylated forms of connexin43. The membranes were washed, developed using electrogenerated chemiluminescence (Amersham Pharmacia Biotech), and exposed to Hyperfilm ECL (Amersham Pharmacia Biotech). The quantification was done by scanning in a Kodak camera (Amersham Pharmacia Biotech) and Gel-Pro Analyzer software (Media Cybernetics, Silver Spring, MD). Values reported are optical densities expressed as arbitrary units.

Immunofluorescence. Hearts from SSI and sham mice were obtained 24 hrs after surgery, sectioned into anterior and posterior halves, immediately frozen, and stored at –80°C for immunohistochemical study. Immunolabeling was performed (5-µm-thick sections) using primary antibodies to connexin43 (mouse monoclonal antibody anti-connexin43) and N-cadherin (goat polyclonal antibody anti-N-cadherin, Santa Cruz Biotechnology). Fluorescein-conjugated secondary antibodies, anti-mouse or anti-goat immunoglobulin G

(Vector Laboratories), were used. Omission of the primary antibodies served as negative controls. The mean area and fluorescence intensity (optical density) of immunoreactivity particles of total connexin43 restricted to the intercalated discs and N-cadherin were analyzed with Leica Qwin software (Leica Imaging Systems, Cambridge, UK) in conjunction with a Leica microscope, videocamera, and an online computer. For the comparison of heterogeneity of connexin43 and N-cadherin in SSI and sham hearts, 5–10 randomly selected images of longitudinally oriented myofibers of 0.0093 mm² were captured from each of four left ventricles per group and analyzed. Some sections were also labeled with phalloidin complexed to rhodamine (Alexa Fluor 594 phalloidin, Molecular Probes, Eugene, OR) for visualization of actin.

Transmission Electron Microscopy. Small blocks (1 mm³) of myocardial tissue from the left ventricle free wall from SSI and sham animals were processed for transmission electron microscopy (n = 5). After fixation with 2.5% glutaraldehyde in cacodylate buffer (pH 7.3) for 2 hrs and postfixation with osmium tetroxide for 2 hrs, the fragments were dehydrated in ascending concentrations of acetone and embedded in araldite. Ultrathin sections were obtained from selected areas with a diamond knife in a Sorvall MT-5000 ultramicrotome (DuPont, Wilmington, DE), double-stained with uranyl acetate and lead citrate, and examined in a Zeiss EM109/900 electron microscope (Carl Zeiss, Oberkochen, Germany) at 80 kV.

Statistical Analysis. The data (except for the survival curves) are reported as the mean ± sd. Multiple comparisons were made using a one-way analysis of variance and Tukey or Bonferroni *post hoc* multiple-comparisons tests. Two groups' comparisons were made using unpaired Student's *t*-test for group data. Bacterial counts were analyzed by the Mann-Whitney U test. The survival rate was expressed as the percentage of live animals. A level of significance of 5% was chosen to denote difference between mean values.

RESULTS

Mortality of Mice Submitted to CLP Sepsis. Figure 1 shows curves of actuarial mortality of the mice submitted to sham operation, MSI, and SSI. Sham-operation animals presented a 100% survival rate through the analyzed period of 72 hrs. The MSI mice showed 90% survival at 12 hrs post injury, declining progressively to 50% survival at 72 hrs. At 24 hrs, defined as the period of study, the survival rate of MSI animals was 80%. The SSI mice showed 70% mortality at 12 hrs after injury, 90% at 24 hrs after injury, and remained steady at this rate until 72 hrs after injury.

Peritoneal Cavity Infection and Bacteremia. Figure 2A shows the number of CFU present in the peritoneal cavity 6 hrs after CLP. MSI mice showed a small number of CFU in the peritoneal cavity, not statically different from the negative number of CFU in sham-operation mice. The mean number of CFU in the peritoneal cavity of SSI mice was higher than that of MSI and sham control animals. Figure 2B shows the number of CFU present in the blood. MSI mice exhibited a mild bacteremia not different from the negative values in the blood of sham con-

trols. The SSI group presented higher bacteremia in comparison with MSI and sham groups.

Carotid Blood Pressure. Figure 3 shows the mean values of carotid blood pressure during the 24-hr period after CLP and sham operation. Mean blood pressure simulating time 0 of the experiment, immediately after surgery, were similar for sham mice (120.20 ± 7.23 mm Hg), MSI mice (114.70 ± 7.67 mm Hg), and SSI mice (117.60 ± 6.95 mm Hg). At 6 hrs after the surgical procedure, the carotid blood pressure was signifi-

cantly lower in MSI and SSI mice (85.42 ± 16.69 mm Hg and 54.29 ± 12.34 mm Hg, respectively), as compared with sham-operation mice (118.90 ± 5.64 mm Hg). At 12 hrs after surgery, the carotid blood pressure in MSI and SSI mice (85.57 ± 14.35 mm Hg and 47.43 ± 12.84 mm Hg, respectively) was significantly lower in comparison with the carotid blood pressure in sham mice (117.80 ± 4.71 mm Hg). At the end of the period of evaluation (24 hrs), the carotid blood pressure in MSI and sham mice was similar (119.20 ± 8.64 mm Hg and 109.60 ± 9.31 mm Hg, respectively). The carotid blood pressure in SSI mice after 24 hrs of observation was 65.86 ± 23.02 mm Hg.

Peritoneal Exudate and Serum Cytokine and Chemokine Levels. Figure 4 shows the concentrations of $\text{TNF}\alpha$ and MIP-1 α in the peritoneal exudate and serum 6 hrs after surgery in sham-operation, MSI, and SSI mice. The $\text{TNF}\alpha$ levels in peritoneal exudate and serum in MSI mice were not different from those in sham controls. In the SSI mice, the peritoneal cavity and serum $\text{TNF}\alpha$ concentrations were markedly increased in comparison with MSI and sham mice. The levels of MIP-1 α in MSI mice were significantly higher in the peritoneal exudate as compared with sham animals, whereas the serum levels of this chemokine were not different. The peritoneal and serum MIP-1 α concentrations were markedly increased in SSI mice in comparison with both MSI and sham-operation mice.

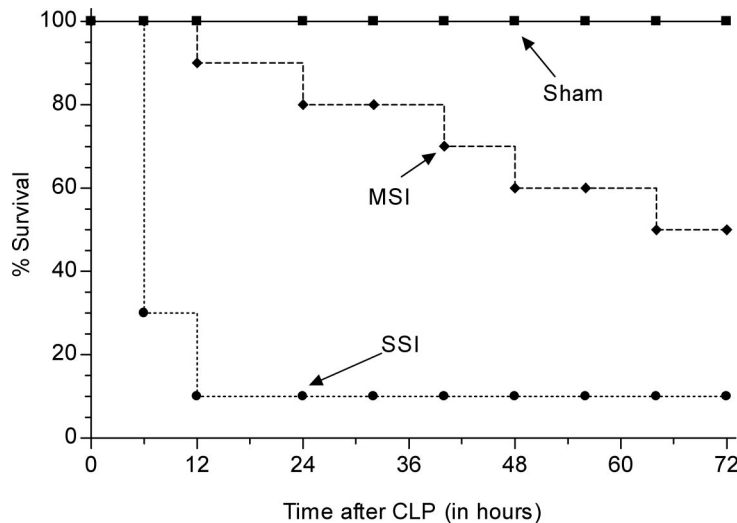


Figure 1. Mortality of the mice submitted to cecal ligation and puncture (CLP) sepsis. Curves of actuarial mortality of mice submitted to sham operation and moderate (MSI) and severe (SSI) septic injury induced by CLP. The survival rate was determined daily until 5 days after surgery. Results are expressed as percentage survival ($n = 10$) and are representative of three different experiments. Survival in the SSI group was significantly different from that in the MSI and sham-operation groups.

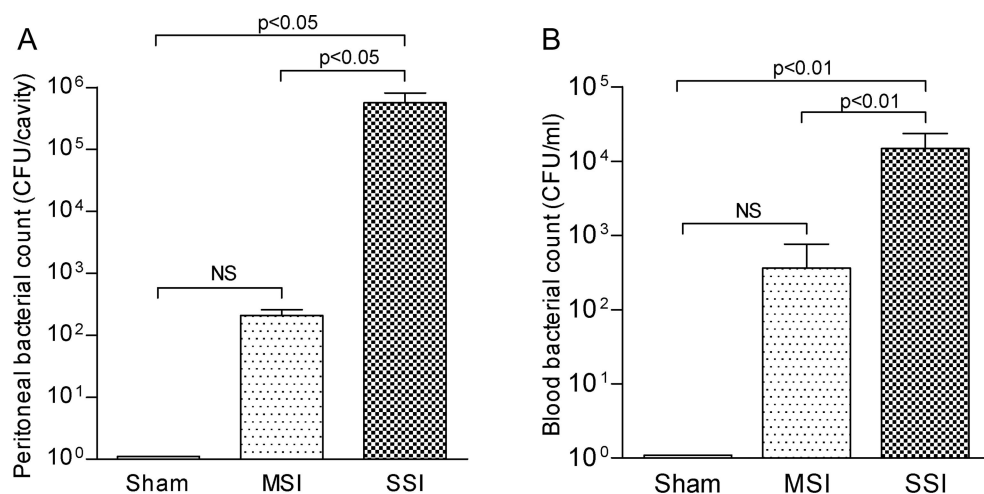


Figure 2. Peritoneal cavity infection and bacteremia. The number of colony-forming units (CFU) in the peritoneal cavity (A) and serum (B) of mice submitted to sham operation and moderate (MSI) and severe (SSI) septic injury induced by cecal ligation and puncture were evaluated 6 hrs after surgery. Results are expressed as mean number of CFU per cavity or CFU per milliliter of blood ($n = 10$) and are representative of three different experiments. The mean number of CFU in the peritoneal cavity of SSI mice was higher than that of MSI and sham control animals.

Western Blot of Connexin43 and N-Cadherin. Figure 5 shows the amounts of connexin43 and N-cadherin 24 hrs after CLP or sham operation expressed in ar-

bitrary units (AU) and representative blots. The amount of connexin43 in SSI mice heart ventricles (658.90 ± 14.80 AU) was markedly reduced as compared

with MSI (1420.00 ± 34.15 AU) and sham-operation (1380.00 ± 75.24 AU) heart ventricles. In contrast, N-cadherin was markedly decreased in both MSI (798.20 ± 74.92 AU) and SSI (660.60 ± 146.30 AU) heart ventricles in comparison with sham-operation heart ventricles (1424.00 ± 487.60 AU).

Immunofluorescent Analysis of Connexin43 and N-Cadherin. The immunohistochemical analysis showed that levels of immunofluorescent signal for connexin43 and N-cadherin were strikingly reduced in left ventricles of hearts from SSI mice, whereas heart ventricles from sham-operation mice showed abundant junctional signal for both proteins (Fig. 6).

The mean area (in percentage) and fluorescent intensity (optical density expressed in arbitrary units, OD) of connexin43 in left ventricles of hearts from SSI mice ($1.18\% \pm 0.20\%$ and 9.80 ± 0.76 OD, respectively) were strikingly decreased as compared with the values in the left ventricles of sham-operation mice ($2.25\% \pm 0.21\%$ and 16.04 ± 0.78 OD, respectively). The mean area and fluorescent intensity of N-cadherin in the left

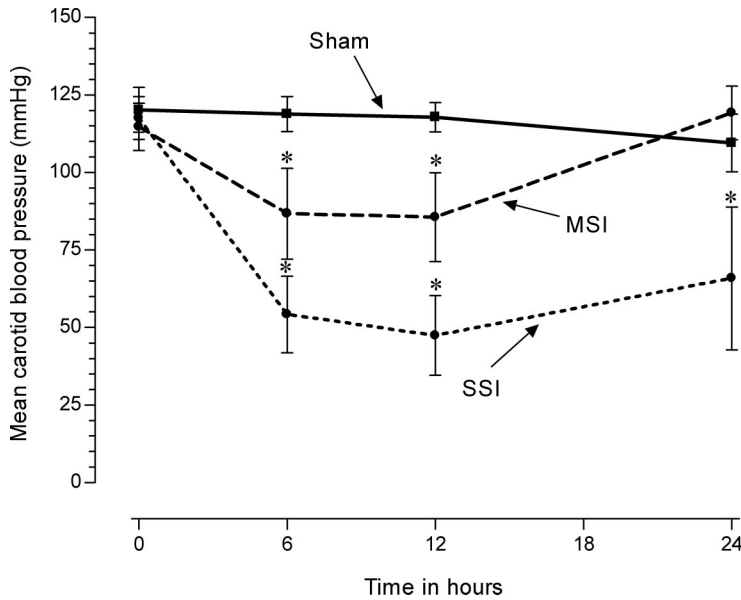


Figure 3. Carotid blood pressure. Mean values of carotid blood pressure at 0, 6, 12, and 24 hrs after sham operation or moderate (MSI) and severe (SSI) septic injury induced by cecal ligation and puncture. The number of animals is six to ten for each group at each time.

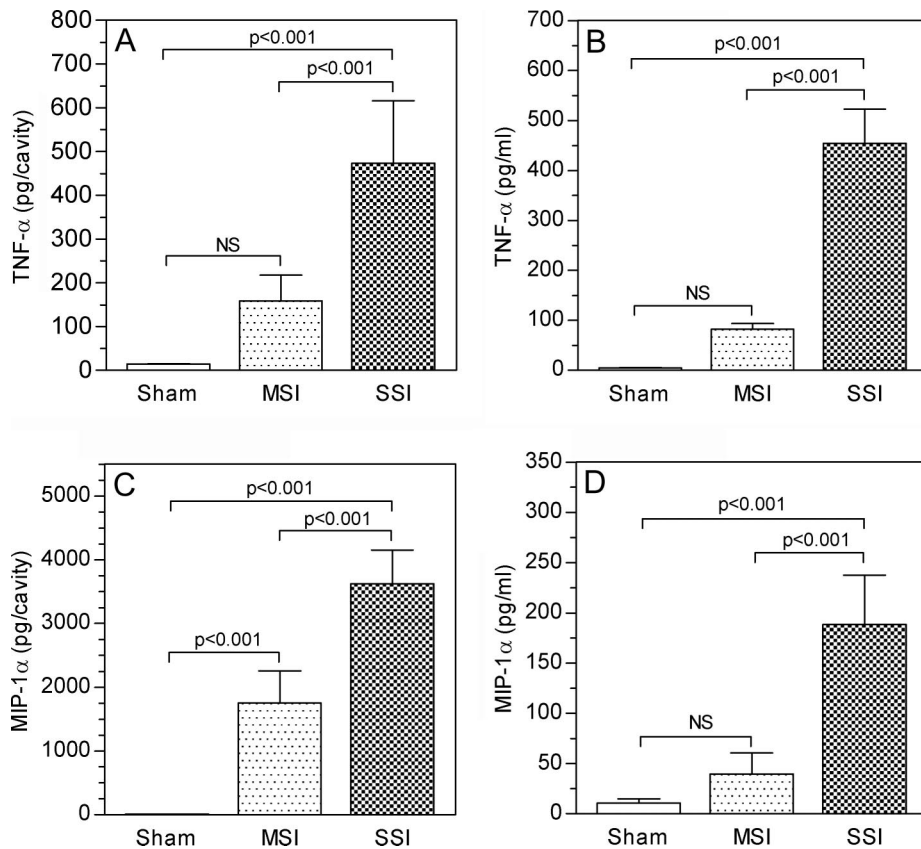


Figure 4. Peritoneal exudate and serum cytokine and chemokine levels. The concentrations of tumor necrosis factor (TNF)- α (A, B) and monocyte inflammatory protein (MIP)-1 α (C, D) were quantified in peritoneal exudates (A, C) and serum (B, D) 6 hrs after surgery in sham-operation, moderate septic injury (MSI), and severe septic injury (SSI) mice. Results (n = 10) are representative of three different experiments. NS, not significant.

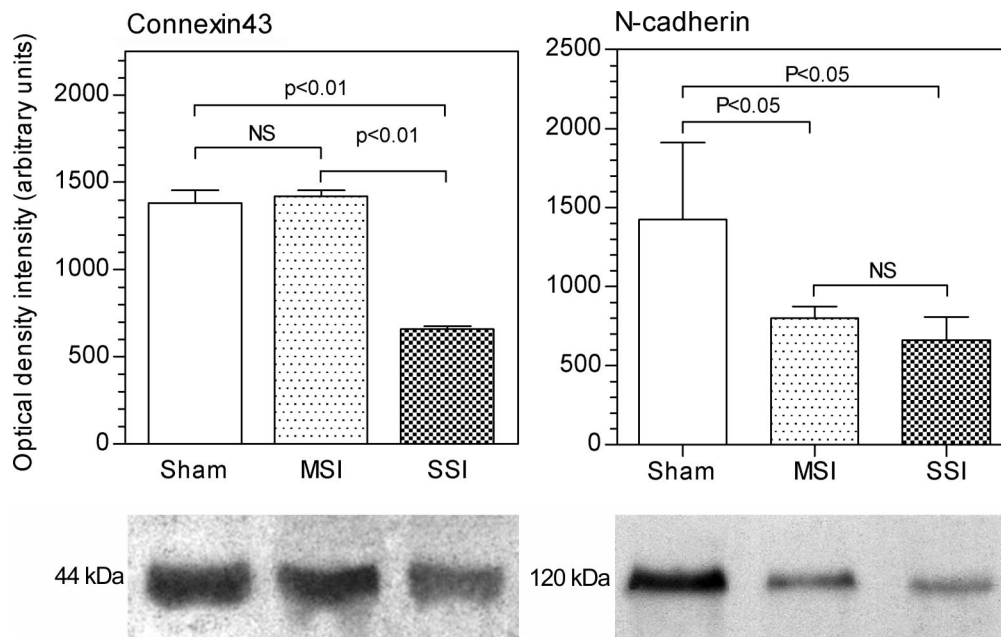


Figure 5. Western blot analysis of connexin43 and N-cadherin. The amounts of connexin43 and N-cadherin of mice submitted to sham operation and moderate (MSI) and severe (SSI) septic injury induced by cecal ligation and puncture (CLP) were measured 24 hrs after surgery and expressed in arbitrary units (AU). Results (n = 6) are representative of three different experiments. NS, not significant.

ventricles of SSI mice ($1.14\% \pm 0.17\%$ and 18.51 ± 2.88 OD, respectively) were strikingly decreased as compared with the values in the left ventricles of sham-operation mice ($2.72\% \pm 0.95\%$ and 27.27 ± 4.17 OD, respectively). Box and whisker-plot graphs show the batches of data in SSI and sham mice regarding the percentage area of connexin43 and N-cadherin signals (Fig. 6).

Dehiscence of Gap and Adherens Junctions in Septic Hearts. The intercalated discs in the myocardium of sham-operation mice did not differ from that reported in the literature. In contrast, a proportion of 30–50% of intercalated discs in SSI mice left ventricular myocardium appeared partly dehiscent or separated (Fig. 7). This dehiscence implicated both adherens and gap junctions.

DISCUSSION

The model of CLP in rodents has been widely used for the investigation of several aspects of sepsis and septic shock (12). In this model, autochthonous gut flora is seeded into the systemic circulation from a septic focus. Because females are better able to tolerate sepsis (13) and endotoxemia (14), to avoid differences between sexes, only male mice were analyzed.

In the present study, the animals submitted to SSI showed a high mortality throughout the analyzed period (72 hrs),

which remained steady at 10% survival after 12 hrs. In comparison, animals submitted to MSI displayed a lower mortality, varying from 90% survival at 12 hrs to 50% survival at 72 hrs. The SSI mice showed a 10% survival in the first 24 hrs after injury, in striking contrast to the 80% survival of the MSI mice. The sham-operation mice showed 100% survival throughout the analyzed period.

The peritoneal cavity and blood cultures 6 hrs after cecal puncture were significantly positive in SSI mice, in contrast to MSI mice, which presented a very low number of CFU in the peritoneal cavity and blood not statistically different from sham-operation controls, which had negative peritoneal cavity and blood cultures.

The mean arterial blood pressure was significantly lower in SSI and MSI mice 6 hrs (reduced by 54.3% and 28.2%, respectively) and 12 hrs (reduced by 59.7% and 27.3%, respectively) after injury as compared with sham-operation controls. At 24 hrs postinjury, the mean arterial blood pressure of SSI mice was lower than that observed in MSI and control mice (reduced by 44.8% and 39.9%, respectively) as long as the mean arterial pressures of MSI and sham-operation mice were not statistically different.

The measurements obtained by peritoneal lavage and serum TNF α expression measured 6 hrs after injury was significantly

higher in SSI mice as compared with MSI and sham mice. The cytokine levels in MSI mice were not significantly different from the levels observed in sham-operation animals. Peritoneal lavage and serum MIP-1 α expression measured 6 hrs after injury were significantly higher in SSI mice as compared with MSI and sham mice. The peritoneal lavage MIP-1 α levels in MSI mice were higher in comparison with those in sham mice, whereas the serum levels were not different from the values observed in controls. TNF α is a prototypical proinflammatory cytokine that has been implicated in the morbidity and mortality associated with septic shock (15–17). The pathogenesis of cardiac dysfunction has been greatly attributed to the myocardial effects of circulating or local TNF α (18). *In vitro* and *in vivo* studies demonstrated that TNF α induces early (19–21) and delayed prolonged (22) myocardial depressant effect. Recent study from our laboratory has demonstrated increased expression of TNF α in the myocardium of human septic hearts, localized to myocytes, interstitial macrophage-type cells, and endothelial and smooth muscle cells in the vessels (11). TNF α -induced myocardial depression involves attenuation of the force of contraction of the individual cardiomyocytes through decreased cytosolic calcium release and decreased myofilament sensitivity to calcium mediated by

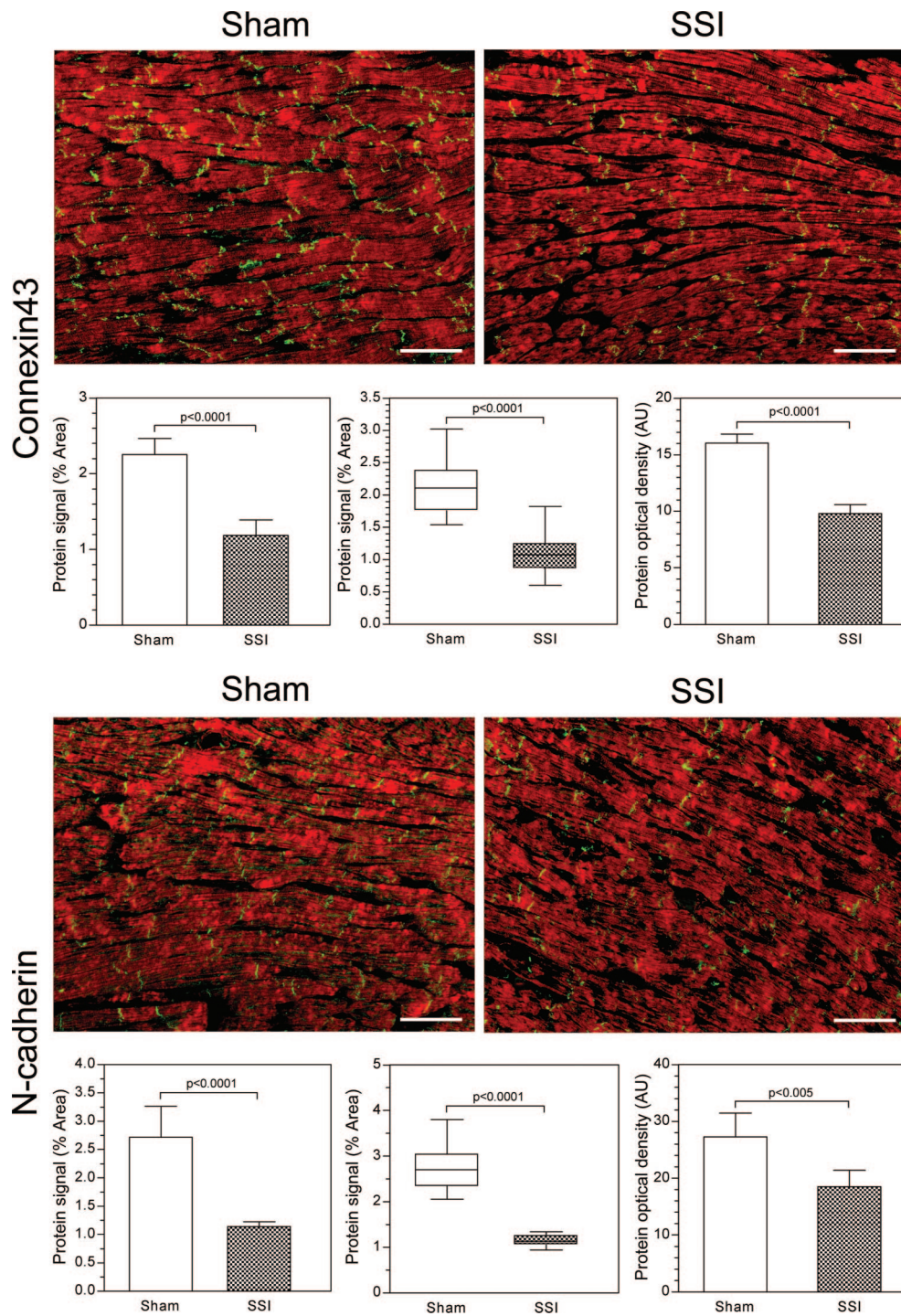


Figure 6. Immunofluorescence analysis of connexin43 and N-cadherin. The immunofluorescent signal for connexin43 and N-cadherin are strikingly reduced in myocardium of mice with severe septic injury (SSI) (right, top and bottom immunohistochemical panels) in comparison with the immunofluorescent signal in sham-operation myocardium (left, top and bottom immunohistochemical panels). The mean area (percentage) and fluorescent intensity (optical density expressed in arbitrary units) of connexin43 and N-cadherin in the left ventricles of SSI mice are markedly decreased as compared with the values in the left ventricles of sham mice. The middle graphs show the batches of data of percentage area of connexin43 and N-cadherin signals. In the immunohistochemical panels, the bars indicate 50 μ m.

high levels of nitric oxide produced by inducible nitric oxide synthase (23). Consonantly, MIP-1 α , a member of the CC chemokines family, has been shown to exert significant activating and chemotactic effect on macrophages, including

their release of TNF α , and, unlike other members of the family, seems to regulate polymorphonuclear function (24, 25).

Western blot analysis of connexin43 expression presented a marked decrease of this junctional protein in the hearts of mice

submitted to SSI as compared with mice submitted to MSI and sham operation (reduced by 52.3% and 53.6%, respectively). Connexin43 protein expressions in MSI and sham hearts were similar. In addition, Western blot analysis of N-cadherin

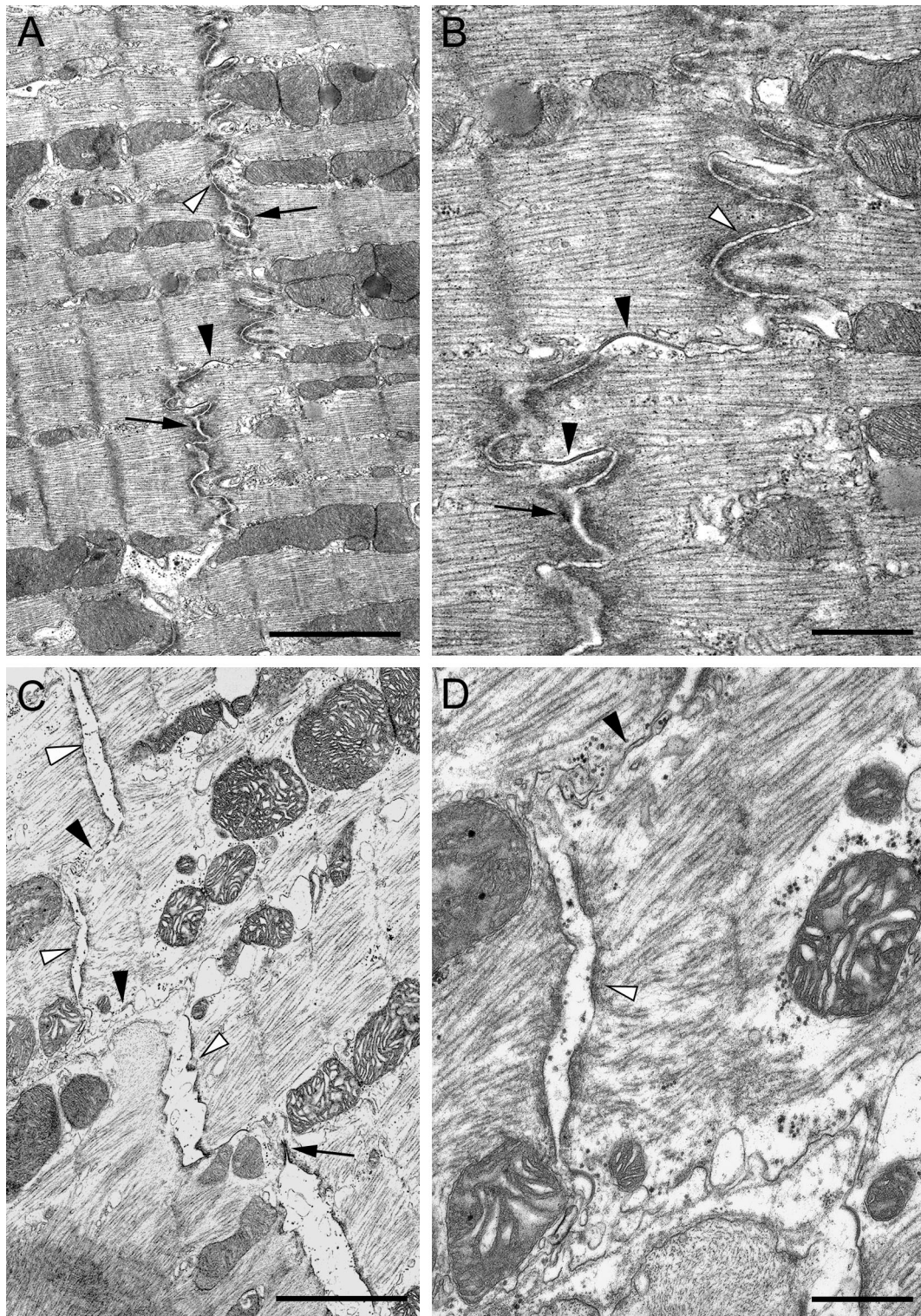


Figure 7. Dehiscence of gap and adherens junctions in septic hearts. The intercalated discs in the myocardium of sham-operation mice did not differ from that reported in the literature (A, B). In contrast, a proportion of 30–50% of intercalated discs in left ventricular myocardium of mice with severe septic injury (SSI) appeared partly dehiscent or separated (C, D). This dehiscence implicated both adherens and gap junctions. Gap junctions are indicated by *black arrowheads*; adherens junctions are indicated by *white arrowheads*; desmosomes are indicated by the *arrow*. In A and C, the *bar* indicates 2 μm ; in B and D, the *bar* indicates 0.5 μm .

showed that the expression of this junctional protein was markedly decreased in the hearts of both SSI and MSI mice in comparison with its expression in the

hearts of sham-operation mice (reduced by 53.2% and 43.9%, respectively).

Immunofluorescence analysis indicated loss of both N-cadherin and con-

nexin43 in SSI induced by CLP in mice. More specifically, immunofluorescence revealed that the areas and the mean intensities (optical density) of both con-

nexin43 and N-cadherin reactive particles at the intercalated discs decreased and the immunopositive spots were sparse. The mean area of connexin43 decreased 47.5%, whereas the mean optical density decreased 38.9%. The mean area of N-cadherin decreased 57.9%, whereas the mean optical density decreased 32.1%. This finding suggests that the number of connexin43 gap junctions' channels decreased in septic hearts. Furthermore, the partial separation of gap junctions observed in the electron microscopic study may be due to the disassembly of the connexin43 complexes, thereby impairing the direct communication between two adjacent cells in septic hearts. The decreased expression of N-cadherin, the principal adherens junction protein primarily localized to intercalated discs, where it serves as attachment site for myofibrils in addition to its structural role in maintaining myocyte adhesion, would alter the stoichiometric relation of the cadherin/myofibril connection. This would disturb the adhesion zipper of the adherens junctions of the intercalated discs in the septic hearts, as observed under the electron microscope, potentially leading to less efficient force transduction across the plasma membrane.

To our knowledge, this is the first study of changes of connexin43 and N-cadherin proteins expression in septic myocardium. A significant depression of connexin43 messenger RNA levels in the myocardium of rats after endotoxemia induced by injection of lipopolysaccharide or after regional hepatic ischemia/reperfusion was previously demonstrated (26). Moreover, based on *in vitro* experiments with a rat myoblast cell line of cardiac origin (H9c2), these authors suggested that the high levels of TNF α detected in the serum of lipopolysaccharide-treated rats could reduce the promoter activity of the connexin43 gene transfected to these cells. The decreased expression of connexin43 in the hearts of mice submitted to severe CLP sepsis may be attributable, at least in part, to the high serum levels of TNF α . This effect may be a contributory factor in the promotion of cardiac depression by TNF α through reduction of electrical/chemical coupling of cardiomyocytes.

The variables analyzed 6 hrs after CLP, number of bacteria in the peritoneal cavity and blood and chemokine measurements, were carried out to characterize the septic process. They represent the first effects of the injurious influence at

the molecular or biochemical level. The variables analyzed 24 hrs after CLP, the amounts of connexin43 and N-cadherin evaluated by Western blot and immunofluorescence and the intercalated disc ultrastructural changes, represent the morphologic consequences of the injurious influence. All stresses and injurious influences exert their effects first at the molecular or biochemical level. There is a lag between the stress and the morphologic changes of cell injury or death. The duration of this delay varies according to the sensitivity of the methods used to detect the changes. The morphologic changes in the present study were only detected in the late periods of the septic process, 18–24 hrs after injury. Because marked and persistent low blood pressure is a hallmark of sepsis/septic shock, the measurement of carotid blood pressure was performed during all of the experimental period: immediately before injury, at 0 hr, and at 6, 12, and 24 hrs after injury.

The functional consequences of our findings are not clear at this moment because we do not know whether the loss of expression of both heart ventricular connexin43 localized to the intercalated discs and N-cadherin caused electrical/chemical and mechanical cell-to-cell coupling impairment. However, the occurrence of hypotension and circulatory shock in septic mice suggests myocardial depression. It could be argued that cardiac dilation caused by other mechanisms leads to the intercalated disc remodeling and thus precedes the observed changes. The hearts of SSI mice 24 hrs after injury were not dilated in comparison with sham-operation controls: the wet heart weights, the left ventricular wall thicknesses, and the left ventricle chamber areas (midventricular coronal section) were similar in both groups (data not shown). Previous study has demonstrated that widespread ventricular myocardial loss of connexin43 in knockout mice produces a highly arrhythmogenic substrate with spontaneous sudden cardiac death and conduction-velocity slowing (5, 6, 8). A reduced expression of connexin43 in ventricular myocardium has been shown in failing, hypertrophied, and ischemic hearts (27–29). Myocardial ischemia leads to connexin43 dephosphorylation and loss of localization to the intercalated disc, which very likely contributes to contractile failure and arrhythmias (30). More recently, an impairment of the conduction in streptozotocin-induced diabetic rat heart has been ascribed to a

decreased expression of connexin43 in the gap junctions' channels (31). We also show a significant decreased expression of N-cadherin protein in the hearts of mice submitted to SSI. As adherens junction is involved in maintaining attachments between adjacent myocardial fibers, the decreased expression of N-cadherin may have an implication on the cell-to-cell adhesion, thus altering the contractile force across the plasma membrane. Recent study using a conditional N-cadherin knockout mice model showed that the animals developed a modest dilated cardiomyopathy with interstitial fibrosis and died of cardiac arrhythmia (4). The authors suggested that the increased interstitial collagen deposition in N-cadherin knockout mice depends on β 1-integrin overexpression increasing cell–extracellular matrix interaction as a response to loss of N-cadherin linkage to the actin cytoskeleton. In addition, the loss of N-cadherin expression resulted in the ensuing decrease of connexin43, thus supporting the view that, to some extent, connexin43 expression is dependent on N-cadherin expression (4, 32, 33). The decreased expression of N-cadherin and connexin43 protein in the myocardium of septic mice may be, in a way, interrelated: our findings showing decreased expression of N-cadherin in SSI and MSI mice hearts in contrast to decreased expression of connexin43 only in SSI mice hearts may represent an additional support to this hypothesis.

An important question is “what is the mechanism of reduction of gap and adherens junction proteins and intercalated disc structural remodeling in the hearts of mice submitted to severe CLP sepsis?” Recent study demonstrated reduction and redistribution of connexin43 and N-cadherin after ischemia and reperfusion using Langendorff-perfused rabbit hearts (33). Considering that the hallmark of septic shock is a dysfunctional microcirculation that produces regional flow disturbances and abnormal tissue oxygenation (34–36), the reduction of connexin43 and N-cadherin and consequent intercalated disc structural remodeling in septic mouse myocardium may be attributed to global ischemia. In addition, taking into account that calcium depletion causes partial separation of cardiomyocytes at intercalated discs (37) and that TNF α impairs intracellular calcium homeostasis (38), this cytokine may also be involved in the pathogenesis of the intercalated disc changes in septic myocardium. These changes are very

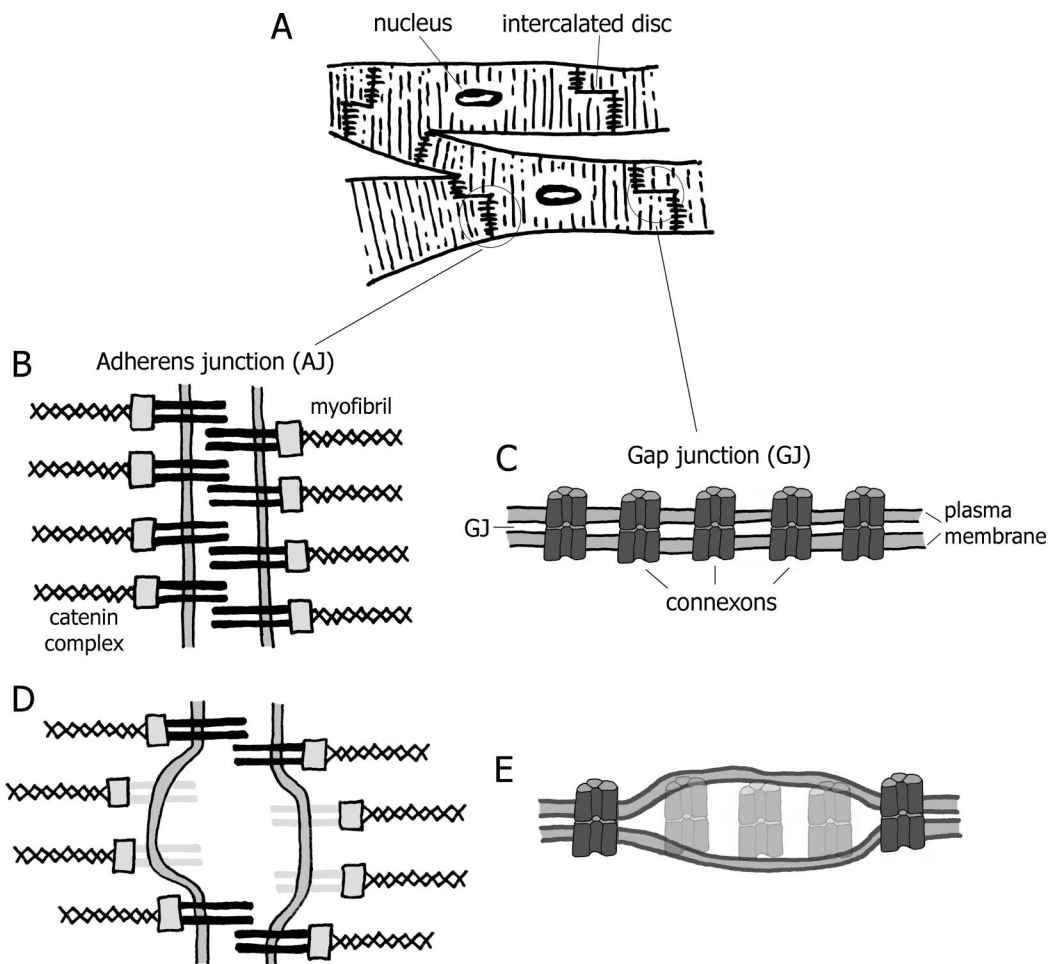


Figure 8. Schematic diagrams representing how N-cadherin and connexin43 may interfere with the remodeling of adherens junctions and gap junctions in septic hearts. In myocardium of mice that underwent sham operation, intercalated disc N-cadherin of the adherens junction, represented by *black bars*, interact to form a strong zipper structure critical to cell-to-cell adhesion. In the myocardium of septic mice, the decreased expression of N-cadherin (missing N-cadherin represented by *gray bars*) promotes the formation of a weak zipper structure, schematically represented as dehiscent per the findings of electron microscopy. In the myocardium of mice that underwent sham operation, six connexin43 polypeptides (in the schematic drawing, only three are represented) form a hemichannel in the membrane of each cell to establish a functional gap junction channel (connexon). In the septic myocardium, the decreased expression of connexin43 (missing connexons represented in *gray*) allows the dehiscence of the gap junction schematically represented in accordance with findings of electron microscopy.

likely reversible and associated with nonlethal or a reversible injury of cardiomyocytes characterized by cell swelling, the so-called hydropic or vacuolar degeneration, clearly reflecting disturbance of membrane function (data not shown). Loss of cell membrane integrity and the resulting exchange of constituents of intracellular and extracellular space as ions and proteins is considered a sign of cell injury. It is, however, difficult to define the stage beyond which the cell is irreversibly damaged and condemned to death.

In conclusion, our data provide important insight regarding the alterations in intercalated disc components resulting from SSI. In this study, significant decrease of key gap and adherens junction proteins (connexin43 and N-cadherin, respectively) resulted in

loss of intercalated disc structural integrity, which may be partly responsible for sepsis-induced cardiac depression. Figure 8 shows schematic diagrams representing how N-cadherin and connexin43 may interfere with the remodeling of adherens junctions and gap junctions in septic hearts. These abnormal variables may emerge as therapeutic targets, and their modulation might provide beneficial effects on future cardiovascular outcomes and mortality in sepsis.

ACKNOWLEDGMENTS

We thank Monica A. Abreu, Lígia B. Santoro, and Maria Elena Riul for excellent technical assistance.

REFERENCES

- Severs NJ: The cardiac muscle cell. *Bioessays* 2000; 22:188–199
- Gutstein DE, Liu F-Y, Meyers MB, et al: The organization of adherens junctions and desmosomes at the cardiac intercalated disc is independent of gap junctions. *J Cell Sci* 2002; 116:875–885
- Perriard JC, Hirschy A, Ehler E: Dilated cardiomyopathy: A disease of the intercalated disc? *Trends Cardiovasc Med* 2003; 13:30–38
- Kostetskii I, Li J, Xiong Y, et al: Induced deletion of the N-cadherin gene in the heart leads to dissolution of the intercalated disc structure. *Circ Res* 2005; 96:346–354
- Gutstein DE, Morley GE, Tamaddon H, et al: Conduction slowing and sudden arrhythmic death in mice with cardiac-restricted inactivation of connexin43. *Circ Res* 2001; 88: 333–339
- Danik SB, Liu FL, Suk J, et al: Modulation of

- cardiac gap junction expression and arrhythmic susceptibility. *Circ Res* 2004; 95: 1035–1041
7. Eckardt D, Theis M, Degen J, et al: Functional role of connexin43 gap junction channels in adult mouse heart assessed by inducible gene deletion. *J Mol Cell Cardiol* 2004; 36:101–110
 8. Van Rijen HV, Eckardt D, Degen J, et al: Slow conduction and enhanced anisotropy increase the propensity for ventricular tachyarrhythmias in adult mice with induced deletion of connexin43. *Circulation* 2004; 109: 1048–1055
 9. Kaplan SR, Gard JJ, Ptoonotarios N, et al: Remodeling of myocyte gap junctions in arrhythmogenic right ventricular cardiomyopathy due to a deletion in plakoglobin (Naxos disease). *Heart Rhythm* 2004; 1:3–11
 10. Feltes TF, Pignatelli R, Leinert S, et al: Quantitated left ventricular systolic mechanics in children with septic shock utilizing noninvasive wall-stress analysis. *Crit Care Med* 1994; 22:1647–1648
 11. Rossi MA, Celes MR, Prado CM, et al: Myocardial structural changes in long-term human severe sepsis/septic shock may be responsible for cardiac dysfunction. *Shock* 2007; 27:10–18
 12. Hubbard WJ, Choudhry M, Schwacha MG, et al: Cecal ligation and puncture. *Shock* 2005; 24(Suppl 1):52–57
 13. Zellweger R, Wichmann MW, Ayala A, et al: Female in proestrus state maintain splenic immune functions and tolerate sepsis better than males. *Crit Care Med* 1997; 25:106–110
 14. Pitcher JM, Wang M, Tsai BM, et al: Endogenous estrogen mediates a higher threshold for endotoxin-induced myocardial protection in females. *Am J Physiol Reg Integr Com Physiol* 2006; 290:R27–R33
 15. Pittet O, Rangel-Frausto MS, Li N, et al: Systemic inflammatory response syndrome, sepsis, severe sepsis and septic shock: Incidence, morbidities are outcomes in surgical ICU patients. *Intensive Care Med* 1995; 21: 302–309
 16. Rangel-Frausto MS, Pittet O, Castigan M, et al: The natural history of systemic inflammatory response syndrome (SIRS): A prospective study. *JAMA* 1995; 273:117–123
 17. Walley KR, Lukacs NW, Standiford TJ, et al: Balance of inflammatory cytokines related to severity and mortality of murine sepsis. *Infect Immun* 1996; 64:4733–4738
 18. Kumar A, Krieger A, Symeonides S, et al: Myocardial dysfunction in septic shock: Part II. Role of cytokines and nitric oxide. *J Cardiothorac Vasc Anesth* 2001; 15:485–511
 19. Finkel MS, Oddis CV, Jacob TD, et al: Negative inotropic effects of cytokines on the heart are mediated by nitric oxide. *Science* 1992; 257:387–389
 20. Walley KR, Herbert PC, Wakai Y, et al: Decrease in left ventricular contractility after tumor necrosis factor- α infusion in dogs. *J Appl Physiol* 1994; 76:1060–1067
 21. Sugishita K, Kinugawa K, Shimizu T, et al: Cellular basis for the acute inhibitory effect of IL-6 and TNF- α on excitation-contraction coupling. *J Mol Cell Cardiol* 1999; 31:1457–1467
 22. De Meules JE, Pigula FA, Mueller M, et al: Tumor necrosis factor and cardiac function. *J Trauma* 1992; 32:686–692
 23. Meldrum DR: Tumor necrosis factor in the heart. *Am J Physiol* 1998; 274:R577–R595
 24. Standiford TJ, Kunkel SL, Lukacs NW, et al: Macrophage inflammatory protein-1 α mediates lung leukocyte recruitment, lung capillary leak, and early mortality in murine endotoxemia. *J Immunol* 1995; 155:1515–1524
 25. Speyer CL, Gao H, Rancillo NJ, et al: Novel chemokine responsiveness and mobilization of neutrophils during sepsis. *Am J Pathol* 2004; 165:2187–2196
 26. Fernandez-Cobo M, Gingalewski C, Drujan D, et al: Downregulation of connexin 43 gene expression in rat heart during inflammation: The role of tumor necrosis factor. *Cytokine* 1999; 3:216–224
 27. Wang X, Gerdes AM: Chronic pressures overload hypertrophy and failure in guinea pigs: III. Intercalated disc remodeling. *J Mol Cell Cardiol* 1999; 31:333–343
 28. Kostin S, Rieger M, Dammer S, et al: Gap junction remodeling and altered connexin43 expression in failing human heart. *Mol Cell Biochem* 2003; 242:135–144
 29. Peters NS, Green PA, Poole-Wilson NJ: Reduced content of connexin43 gap junctions in ventricular myocardium from hypertrophied and ischemic human heart. *Circulation* 1993; 88:864–875
 30. Beardslee MA, Lerner DL, Tadros PN, et al: Dephosphorylation and intracellular redistribution of ventricular connexin43 during electrical uncoupling induced by ischemia. *Circ Res* 2000; 87:656–662
 31. Lin H, Ogawa K, Imanaga I, et al: Remodeling of connexin43 in the diabetic rat heart. *Mol Cell Biochem* 2006; 290:69–78
 32. Li J, Patel VV, Radice GL: Dysregulation of cell adhesion proteins and cardiac arrhythmogenesis. *Clin Med Res* 2006; 4:42–52
 33. Tansey EE, Kwaku KF, Hammer PE, et al: Reduction and redistribution of gap and adherens junction proteins after ischemia and reperfusion. *Ann Thorac Surg* 2006; 82: 1472–1479
 34. Hinshaw LB: Sepsis/septic shock: Participation of the microcirculation: an abbreviated review. *Crit Care Med* 1996; 24:1072–1078
 35. Rossi MA, Santos CS: Sepsis related microvascular myocardial damage with giant cell inflammation and calcification. *Virchows Arch* 2003; 443:87–92
 36. Chagnon F, Bentourkia M, Lecomte R, et al: Endotoxin-induced heart dysfunction in rats: Assessment of myocardial perfusion and permeability and the role of fluid resuscitation. *Crit Care Med* 2006; 34:127–133
 37. Greve G, Rotevatn S, Saetersdal T, et al: Ultrastructural studies of intercalated disc separations in the rat heart during the calcium paradox. *Res Exp Med* 1985; 185: 195–206
 38. Zhang M, Xu YJ, Saini HK, et al: TNF- α as a potential mediator of cardiac dysfunction due to intracellular Ca^{2+} -overload. *Biochem Biophys Res Commun* 2005; 327: 57–63